Three-Dimensional Segmentation and Visualization of Cerebral Arteries and Veins from Simultaneously Acquired MRA and MRV based on Graph-Cuts and Vessel Enhancement Filter

H. Shim[1,2], S-H. Park[1,3], and K. T. Bae[1,3]

[1]Department of Radiology, University of Pittsburgh, Pittsburgh, PA, United States, [2]School of Electrical Engineering, Seoul National University, Seoul, Seoul, Korea, Republic of, [3]Department of Bioengineering, University of Pittsburgh, Pittsburgh, PA, United States

Introduction

Accurate segmentation and appropriate visualization of the arteries and veins in the brain improve the detection and characterization of vascular abnormality such as cerebral aneurysm, arteriovenous malformation and tumor vascularity. Traditional 2D projection display of vascular images such as minimum-intensity projection (minIP) of veins in MRV offers limited visualization of complex vascular structures in the brain. This limitation becomes more problematic when we desire to display both the arteries and veins together that are acquired simultaneously from newly-introduced compatible dual-echo arteriovenography (CODEA). Thus, we propose a new 3D segmentation method to segment the arteries and veins from MRA and MRV in the brain, respectively, using a graph-cuts technique [2] and a vessel enhancement filter [3] and then display the arteries and veins together in 3D.

Material and Methods

The experiments were performed for two normal volunteers on a 3T scanner (Siemens Medical Solutions, Erlangen, Germany) with a vendor-supplied, circularly-polarized head RF coil. The MRA and MRV were simultaneously acquired with the CODEA technique with the scan parameters of TR = 40 ms, TE = 3.2 / 20 ms, acquisition bandwidth = 150 / 50 Hz/pixel, matrix size = 512×192×64, corresponding FOV = 240×180×80 mm^3, and total scan time = 9.8 min. Through an echo-specific K-space reordering scheme, a spatial pre-saturation pulse was selectively applied to MRA (for venous signal suppression) and flip angle of the first echo (MRA) and the second echo (MRV) was separately adjusted to be 25° and 15°, respectively.

The MRA and MRV were separately processed for segmentation of arteries and veins, respectively, with the overall workflow described in Fig. 1. The two main components of this workflow were semi-automated (SA) segmentation using the graph-cuts (GC) technique [2] and enhancement of veins using the Utrecht vessel enhancement filter (VEF) [3] (thick boxes in Fig. 1). The GC SA segmentation process was composed of placement of seeds (Fig. 2c) and computation of the segmentation. These two procedures were iterated until the revised result became acceptable to the user. Whereas we applied only the GC SA segmentation method to the MRA image (GC1 step in Fig. 1), an MRV image requires enhancement of vessels, especially thin vessels. The Utrecht VEF is a well-known method to emphasize tubular structures which are brighter or darker than background. Although veins in an MRV are darker than other brain tissues, the susceptibility artifacts which have dark signals with intensity range similar to veins hinder direct application of the VEF. For that reason, we extracted only the brain parenchyma regions using the GC SA segmentation again (GC2 step in Fig. 1, Fig. 2c) to exclude the artifacts. Then, the VEF with the smallest scale (s=1.0 [3]) was applied to the brain parenchyma region and the thickest veins like sagittal sinus were extracted by simple thresholding (Thr1 step in Fig. 1). The proposed method has several post-processing steps such as connected component analysis (CCA), mathematical morphological operations (MMO) or combination of them. The MMO1 step in Fig. 1, which is an erosion operation with the spherical structuring element of 6-voxel-radius, was aimed to remove most of the artifacts which remained after the GC segmentation. The other steps (CCA1, CCA2, and MMO2) were in order to remove scattered clutter after the segmentation processes. The remaining part of the workflow was devoted to visualization steps, which are denoted as the parallelograms in Fig. 1. The enhancement result of the VEF was visualized by the maximum intensity projection (MIP) technique (Fig. 3a and b) and the segmentation results of arteries and veins were individually visualized by the surface shaded display method (SSD1 and SSD2 steps in Fig. 1, Fig. 4a and b), or altogether with the same method (SSD3 step in Fig. 1, Fig. 4c).

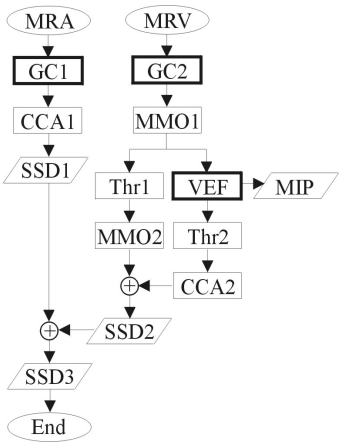

Fig. 1 The overall workflow:
GC (graph-cut segmentation)
VEF (vessel enhancement filter)
Thr (thresholding)
CCA (connected-component analysis)
MMO (mathematical morphological operation)
MIP (maximum intensity projection)
SSD (surface shaded display)

Results and Discussion

Veins with hypo-intensity in the original MRV images could be demonstrated in detail with hyper-intensity after brain parenchyma segmentation (GC2) and vessel enhancement (VEF), allowing comprehension and interpretation of the whole venous structure by use of MIP technique (Fig. 3). The vascular trees were also displayed well using SSD technique (Fig. 4a and b). In addition, the relative position of arterial and venous structures in the whole brain could be interpreted altogether, when the two 3D visualization results were merged together (Fig. 4c).

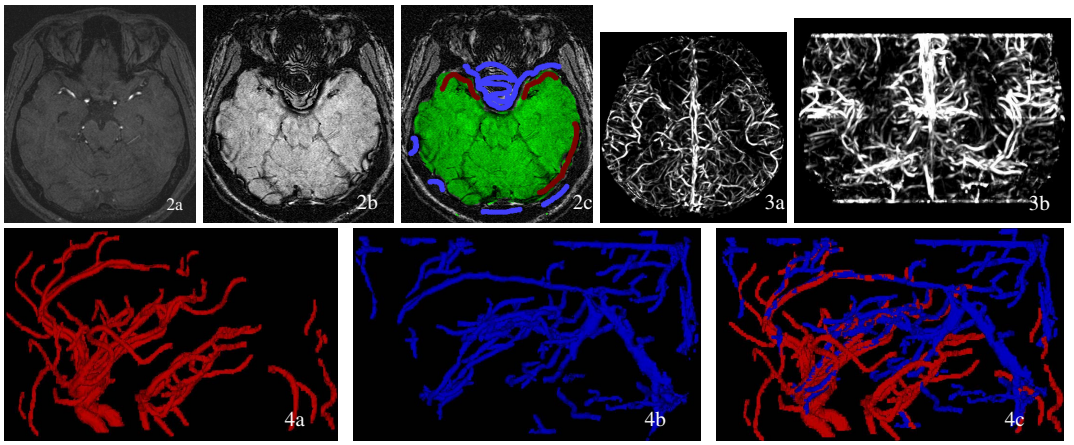

Fig. 2 (a) MRA image (b) MRV image (c) placement of seeds (i.e., red and blue curvilinear marks) and segmented brain parenchyma in green;
Fig. 3 (a,b) MIP representation of the veins enhaced by the VEF which applied to only the brain parenchyma in MRV
Fig. 4 SSD representation of segmented (a) arteries, (b) veins, and (c) both.

In conclusion, our segmentation and visualization scheme in conjunction with the CODEA technique is a promising method, when there is a need to study the morphology of both arteries and veins together in the brain. This method would facilitate the characterization and quantification of vascular abnormalities in the brain. Future works will be dedicated to quantitative evaluation of the vessels in clinical settings of arteriovenous malformation and brain tumor vascularity.

References

[1] Haacke et al., MRM 52:612-618 (2004); [2] Boykov et al., ICCV:105-112 (2001); [3] Frangi et al., MICCAI:130-137 (1998);